# Metabolic profiling of murine plasma reveals an unexpected biomarker in rofecoxib-mediated cardiovascular events

Jun-Yan Liu[a], Ning Li[b], Jun Yang[a], Nan Li[c], Hong Qiu[b], Ding Ai[a,c], Nipavan Chiamvimonvat[b], Yi Zhu[c], and Bruce D. Hammock[a,1]

[a]Department of Entomology and University of California-Davis Cancer Center and [b]Division of Cardiovascular Medicine, University of California, Davis, CA 95616; and [c]Department of Physiology, Beijing University, Beijing 100083, People's Republic of China

Contributed by Bruce D. Hammock, August 6, 2010 (sent for review June 16, 2010)

**Chronic administration of high levels of selective COX-2 inhibitors (coxibs), particularly rofecoxib, valdecoxib, and parecoxib, increases risk for cardiovascular disease. Understanding the possibly multiple mechanisms underlying these adverse cardiovascular events is critical for evaluating the risks and benefits of coxibs and for development of safer coxibs. The current understanding of these mechanisms is likely incomplete. Using a metabolomics approach, we demonstrate that oral administration of rofecoxib for 3 mo results in a greater than 120-fold higher blood level of 20-hydroxyeicosatetraenoic acid (20-HETE), which correlates with a significantly shorter tail bleeding time in a murine model. We tested the hypothesis that this dramatic increase in 20-HETE is attributable to inhibition of its metabolism and that the shortened bleeding time following rofecoxib administration is attributable, in part, to this increase. The s.c. infusion of 20-HETE shortened the tail bleeding time dramatically. Neither 20-HETE biosynthesis nor cytochrome P4A-like immune reactivity was increased by rofecoxib administration, but 20-HETE production increased in vitro with the addition of coxib. 20-HETE is significantly more potent than its COX-mediated metabolites in shortening clotting time in vitro. Furthermore, 20-HETE but not rofecoxib significantly increases rat platelet aggregation in vitro in a dose-dependent manner. These data suggest 20-HETE as a marker of rofecoxib exposure and that inhibition of 20-HETE's degradation by rofecoxib is a partial explanation for its dramatic increase, the shortened bleeding time, and, possibly, the adverse cardiovascular events associated with rofecoxib.**

cardiovascular side effect | coxib | eicosanoids | metabolomics | Vioxx

Rofecoxib (Vioxx), a potent, orally active, and selective COX-2 inhibitor, was approved by the US Food and Drug Administration to treat osteoarthritis, rheumatoid arthritis, acute pain, dysmenorrhea, and migraine on May 20, 1999. Rofecoxib was voluntarily withdrawn from the worldwide market by its manufacturer, Merck, on September 30, 2004 because it was associated with a higher risk for adverse cardiovascular events and stroke in arthritic patients compared with those on the control naproxen (1, 2). This resulted in nearly 27,000 lawsuits involving an almost $5 billion settlement (3). In addition, high doses of other coxibs such as valdecoxib and celecoxib are associated with cardiovascular problems (1, 4).

The dominant theory proposed to explain the cardiovascular events is based on monitoring only a few arachidonate metabolites. Current theory is that rofecoxib reduces the production of the platelet aggregation inhibitor prostacyclin $I_2$ ($PGI_2$), whereas it has much less effect on the production of the potent platelet activator thromboxane (TX) $A_2$ (5, 6). Data generated in this laboratory on $PGI_2/TXA_2$ ratios in inflamed mice are consistent with this hypothesis (7). This would be a common mechanism shared by other selective COX-2 inhibitors. Based on this discovery, one might expect that conventional nonselective nonsteroidal antiinflammatory drugs (NSAIDs) other than coxibs should be neutral or even beneficial to the cardiovascular system. However, a significantly increased risk for cardiovascular diseases such as myocardial infarction (MI), hypertension, and heart failure has also been observed to be associated with the administration of the nonaspirin conventional NSAIDs, including but not limited to diclofenac, ibuprofen, naproxen, and indomethacin (8–12). In addition, there could be rofecoxib-specific events such as the facile formation of a cardiotoxic maleic anhydride derivative from rofecoxib that may contribute to its adverse effects (13). This hypothesis fails to explain the increased risk in the cardiovascular system from other nonaspirin NSAIDs. Thus, current mechanisms provide an incomplete explanation for cardiovascular problems associated with the use of NSAIDs.

To evaluate the risks and benefits of selective COX-2 inhibitors and to develop safe coxibs or adjuvants to improve the safety of existing coxibs, it is critical to understand the possibly multiple mechanisms underlying the adverse cardiovascular events. Previous studies focused on the oxylipin mediators from arachidonic acid (ARA) generated by COX enzymes, which hindered a broader understanding of the mechanism(s) underlying the coxib-mediated cardiovascular events (5, 6). In contrast, in our current study, we used a broader metabolomics approach to quantify the representative oxylipin mediators derived from ARA and linoleic acid (LA) mediated by COXs, lipoxygenases (LOXs), and cytochrome P450s (CYP450s) using liquid chromatography-tandem mass spectrometry (LC-MS/MS) (Fig. S1). Metabolomics is a promising approach that has been widely used as a powerful tool in disease diagnosis (14), biomarker discovery (15), toxicity evaluation (16), gene function (17), and pharmacological research (18, 19). Here, we applied metabolomic profiling to a murine model (20). We present evidence that rofecoxib acts, in part, to accumulate the ARA metabolite 20-hydroxyeicosatetraenoic acid (20-HETE), a potent vasoconstrictor, thus increasing the risk for MI and stroke. This mechanism may be shared with other nonaspirin NSAIDs.

## Results

**Metabolomic Profiling of the Plasma from Mice Chronically Treated with Rofecoxib.** As expected, administration of rofecoxib to mice for 3 mo resulted in a dramatically shortened bleeding time (Fig. 1*A*). Metabolomic profiling of the plasma from treated mice resulted in the quantitative levels of 27 oxylipin mediators (Table S1). The plasma levels of $TXB_2$ and 6-keto-prostaglandin (PG) $F_{1\alpha}$ (the relatively stable metabolites of $TXA_2$ and $PGI_2$, respectively) were under the quantitation limits, as expected, in noninflamed animals. However, an increase of greater than 120-fold was ob-

Author contributions: J.-Y.L., N.C., Y.Z., and B.D.H. designed research; J.-Y.L., Ning Li, J.Y., Nan Li, H.Q., and D.A. performed research; J.-Y.L., Ning Li, J.Y., Nan Li, H.Q., and D.A. analyzed data; and J.-Y.L., N.C., Y.Z., and B.D.H. wrote the paper.

The authors declare no conflict of interest.

[1]To whom correspondence should be addressed. E-mail: bdhammock@ucdavis.edu.

This article contains supporting information online at www.pnas.org/lookup/suppl/doi:10.1073/pnas.1011278107/-/DCSupplemental.

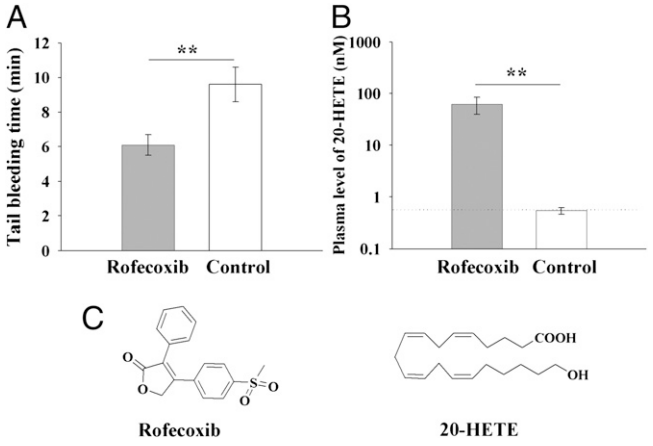


**Fig. 1.** Chronic administration of rofecoxib significantly increases the blood level of 20-HETE, leading to a dramatically shortened tail bleeding time. (*A*) Oral administration of rofecoxib for 3 mo results in a dramatically shortened tail bleeding time ($n = 6$). The tail bleeding time was measured before the mice were killed. If the bleeding time was more than 10 min, the experiment was terminated at 10 min and recorded as 10 min. (*B*) Oral administration of rofecoxib for 3 mo results in a dramatic increase in plasma levels of 20-HETE ($n = 6$; dotted line, quantitative limit). (*C*) Structures of rofecoxib and 20-HETE. Data represent the mean ± SD. Rofecoxib was provided in the drinking water at a concentration of 50 mg/L. The bleeding time is a parameter of blood aggregation. A shorter bleeding time means that the blood is easier to aggregate, which can increase the risk for cardiovascular events. Statistical significance was determined by a two-sided unpaired *t* test and one-way ANOVA (**$P < 0.01$).

served in the plasma concentration of 20-HETE in the mice treated with rofecoxib (Fig. 1 *B* and *C*, and Table S1).

**Effect of 20-HETE Infusion on Murine Bleeding Time.** The s.c. infusion of 20-HETE to mice for 3 wk resulted in a dramatic decrease in bleeding time (Fig. 2*A*). In addition, s.c. infusion of 20-HETE led to a significantly higher level of 20-HETE in murine plasma (Fig. 2*B*).

**Regulation of 20-HETE Production by Rofecoxib and Other COX Inhibitors in Vitro.** Incubation of rofecoxib with ARA in a murine hepatic S-9 fraction shows that rofecoxib increases the production of 20-HETE in a time- and dose-dependent manner (Fig. 3). In addition, both the nonselective COX inhibitor indomethacin and the selective COX-1 inhibitor SC-560 significantly increase the production of 20-HETE (Fig. 3*B*).

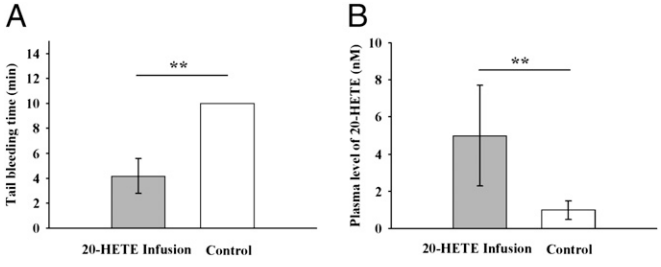


**Fig. 2.** Infusion of 20-HETE significantly shortened the murine tail bleeding time. (*A*) Infusion (s.c.) of 20-HETE for 3 wk leads to a significantly shortened tail bleeding time ($n = 6$). The tail bleeding time was measured before the mice were killed. If the bleeding time was more than 10 min, the experiment was terminated at 10 min and recorded as 10 min. (*B*) Infusion (s.c.) of 20-HETE for 3 wk results in a higher plasma level of 20-HETE ($n = 6$). Data represent the mean ± SD. 20-HETE was administered with s.c. infusion at a flow rate of 250 ng/h. The bleeding time is a parameter of blood coagulation. A shorter bleeding time means that the blood is easier to aggregate, which increases the risk for cardiovascular events. Statistical significance was determined by a two-sided unpaired *t* test and one-way ANOVA (**$P < 0.01$).

**Effects of 20-HETE and Its COX-Mediated Metabolites on Murine Blood Clotting Time in Vitro.** Fig. 4 illustrates the in vitro effects of 20-HETE and two of its COX-mediated metabolites [20-hydroxyl $PGE_2$ (20-OH $PGE_2$) and 20-hydroxyl $PGF_{2\alpha}$ (20-OH $PGF_{2\alpha}$)] on murine blood clotting time (MBCT). 20-HETE significantly shortens the MBCT when compared with a control. In comparison to 20-HETE, 20-OH $PGF_{2\alpha}$ significantly delays the MBCT and 20-OH $PGE_2$ slightly delays MBCT (Fig. 4).

**Effects of 20-HETE and Rofecoxib-Mediated Hemostatic Coagulation on Murine Plasma in Vitro.** To illustrate the mechanism of the delay of MBCT by 20-HETE, prothrombin time (PT), thrombin time (TT), activated partial thromboplastin time (APTT), and plasma fibrinogen (FIB) levels were measured with fresh murine plasma treated with different concentrations of 20-HETE and rofecoxib. The international normalized ratio (INR) was also calculated. As shown in Table S2, neither 20-HETE nor rofecoxib caused significant changes in those indexes of hemostatic coagulation in mice.

**Effects of 20-HETE and Rofecoxib-Mediated Platelet Aggregation on Rat Blood Platelet in Vitro.** Fig. 5 shows the in vitro effects of 20-HETE on ADP-induced platelet aggregation. Because of the limitation of blood volume from mice, the platelet aggregation assay was measured with fresh isolated rat platelets. As shown in Fig. 5*A*, 20-HETE but not rofecoxib significantly increases the content of ADP-induced platelet aggregation when compared with a control, which is dose-dependent starting from $10^{-7}$ M. In addition, 20-HETE accelerates the ADP-induced platelet aggregation rate in a time-related manner (Fig. 5*B*).

## Discussion

Bleeding time roughly reflects platelet aggregability. Increased platelet aggregability has been found to be associated with the pathogenesis of MI (21–23) and stroke (24). In addition, a significantly shorter bleeding time was found in patients with diagnosed MI when compared with patients without MI (25, 26). Thus, tail blood bleeding time was selected as a simple readout for the cardiac risk for chronic administration of rofecoxib in the current study.

A randomized double-blind experiment was conducted in a murine model (protocol 1). After 3 mo of drug administration, as expected, a dramatically shortened tail bleeding time was observed in the animals administered rofecoxib compared with controls (Fig. 1*A*). This increased clotting propensity may contribute to a high incidence of MI and stroke. Many pharmaceutical agents, including rofecoxib, inhibit enzymes in the arachidonate cascade. Previous studies focused on analysis of the ARA metabolites of the COX pathway as markers of administration of rofecoxib and other NSAIDs and on investigation of both the therapeutical effects and side effects of these pharmaceutical agents (5, 6). In contrast, a broader metabolomic profiling strategy was used in current study to analyze murine plasma for the metabolites of the COX, LOX, and CYP450 branches of the arachidonate and linoleate cascades (target analytes illustrated in Fig. S1). Among the detectable oxylipin mediators derived from ARA and LA (Table S1), the most striking and unexpected finding was a dramatically higher level of 20-HETE in the plasma of the mice administrated rofecoxib (Fig. 1*B*).

Although the inhibition of COX-2 by rofecoxib is reversible (27), the increase in 20-HETE was still observed when rofecoxib was incubated with ARA and the hepatic S-9 fraction prepared from the treated animals (Fig. 3). This is consistent with the in vivo observation (Fig. 1*B*). 20-HETE is one of the metabolites of ARA produced by CYP450s (CYP4As and CYP4Fs) (28). One could envision that the 20-HETE increase is attributable to the increased ARA substrate available after COX inhibition. If this were the cause, one could expect other CYP metabolites such as epoxyeicosatrienoic acids (EETs) and dihydroxyeicosatrienoic acids (DHETs) to increase dramatically as well. However, increases in EETs or DHETs were not observed (Table S1). Another expla-

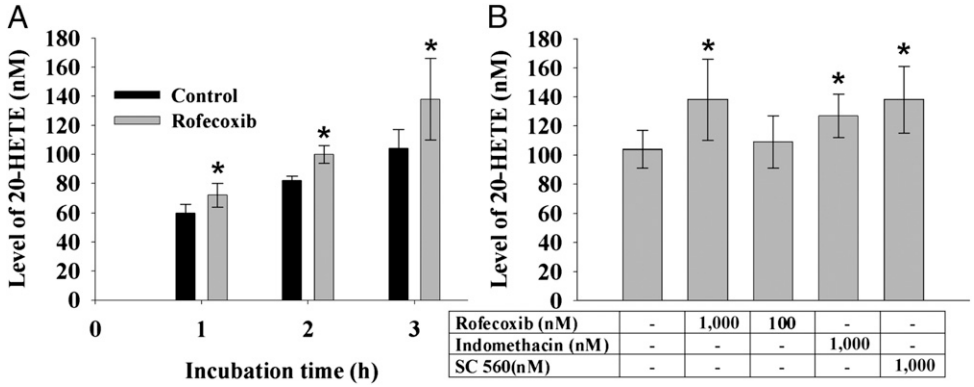


**Fig. 3.** Accumulation of 20-HETE following treatment of murine hepatic S-9 fraction with rofecoxib, SC-560, and indomethacin. (*A*) Significant increase was observed in the production of 20-HETE in a time-related manner following the incubation of normal murine hepatic S-9 fraction and ARA with rofecoxib (1 μM; $n$ = 6). (*B*) Significant increase was observed in the production of 20-HETE following a 3-h incubation of normal murine liver S-9 fraction and ARA with rofecoxib, SC-560, and indomethacin (1 μM each; $n$ = 6), whereas a slight increase was observed with rofecoxib (100 nM; $n$ = 6). Data represent the mean ± SD. Statistical significance was determined by a two-sided unpaired $t$ test and one-way ANOVA (*$P < 0.05$).

nation could be that rofecoxib administration induces the enzymes that catalyze the 20-HETE formation such as CYP4A10, CYP4A12, or CYP4A14. However, Western immunoblot analysis with an anti-rat CYP4A antibody showed that rofecoxib does not alter the expression of related CYPs at the protein level in murine liver (Fig. S2). The fact that the 20-HETE formation rate is not altered by in vivo rofecoxib exposure (Fig. S2 *C* and *D*) argues that biosynthesis of 20-HETE is not altered. 20-HETE has been demonstrated to be further metabolized by COX to 20-hydroxy PGs (e.g., 20-OH-$PGE_2$, 20-OH-$PGF_{2\alpha}$) and other mediators (29–31) in in vitro studies. Thus, the 20-HETE increase both in vivo and in vitro could be explained by blocking one of its major routes of degradative metabolism pathways using rofecoxib. This time- and dose-dependent increase in the production of 20-HETE is demonstrated not only with rofecoxib but with the selective COX-1 inhibitor SC-560 and nonselective COX inhibitor indomethacin (Fig. 3). 20-HETE also is oxidized to 20-COOH-ARA (32). The possibility that rofecoxib and its metabolites such as maleic anhydride (13) could attenuate the oxidization of 20-HETE, and thus result in the accumulation of 20-HETE, was not supported by the significant increase of 20-HETE associated with the selective COX-1 inhibitor SC-560 and the nonselective COX inhibitor indomethacin, which are structurally different from rofecoxib. We propose the hypothesis that the increase in 20-HETE in vivo and in vitro is mainly attributable to the reduction in the metabolism of 20-HETE by the inhibition of COX enzymes that are important in the metabolism of 20-HETE.

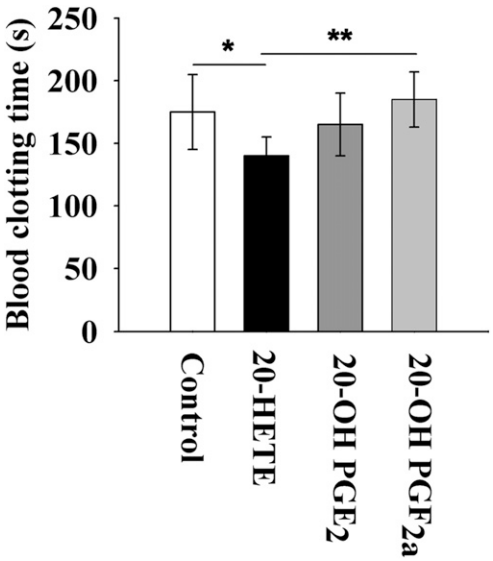


**Fig. 4.** In vitro effects of 20-HETE and its COX-mediated metabolites on blood clotting time. Venous blood (25 μL) was collected from the tail of Swiss Webster mice (male, 8 wk of age) to test blood clotting time using prescored capillary tubes rinsed with DMSO, 20-HETE (0.5 mM in DMSO), 20-OH-$PGE_2$ (0.5 mM in DMSO), or 20-OH-$PGF_{2\alpha}$ (0.5 mM in DMSO). The final concentration of 20-HETE, 20-OH-$PGE_2$, and 20-OH-$PGF_{2\alpha}$ was calculated to be ≈13 μM. Each compound was tested with blood from six individual mice. Data represent the mean ± SD ($n$ = 6). Statistical significance was determined by a two-sided unpaired $t$ test and one-way ANOVA (*$P < 0.05$; **$P < 0.01$).

To test whether 20-HETE contributes to the shortened bleeding time, direct infusion of 20-HETE was performed in mice to explore the possible alteration in bleeding time (protocol 2). After 3 wk of infusion, 20-HETE rose to 5 nM in the murine plasma and dramatically shortened bleeding time (Fig. 2). When compared with chronic administration of rofecoxib, direct infusion of 20-HETE results in a lower plasma level of 20-HETE but a similar effect on shortening bleeding time, which may be attributable to the exposure duration of 20-HETE. This also indicates more complicated mechanism(s) underlying the chronic administration of rofecoxib than those proposed. However, this demonstrates that an increase in 20-HETE contributes to a shortening of bleeding time in vivo. This hypothesis is supported by in vitro assays showing that 20-HETE significantly shortens MBCT (Fig. 4*A*). In addition, we measured the plasma level of FIB and platelet factor 4 (PF-4) for the mice in protocol 2. The results show that infusion of 20-HETE increases the plasma levels of FIB and PF-4 without statistic significance (Fig. S3). In summary, both in vivo and in vitro studies suggest that a higher level of 20-HETE contributes to the enhanced speed of blood clotting associated with chronic administration of rofecoxib. This and other effects of increased 20-HETE such as vasoconstriction may contribute to the occurrence of MI and stroke (33).

An increase in 20-HETE has been documented to be associated with exacerbation of MI and stroke in multiple animal models, and inhibition of the production of 20-HETE decreases the infarct size and ablates strokes in several animal models (34–37). To study the mechanism by which 20-HETE enhances the speed of blood clotting, we measured the function of coagulation and platelet aggregation. We found that 20-HETE significantly increases ADP-induced platelet aggregation but not coagulation. Thus, 20-HETE caused the shortening of bleeding time and blood clotting time as a result of the increase in platelet aggregation rather than dysfunction of coagulation via clotting factors. Previous studies show that 20-HETE is released from human platelet phospholipids on

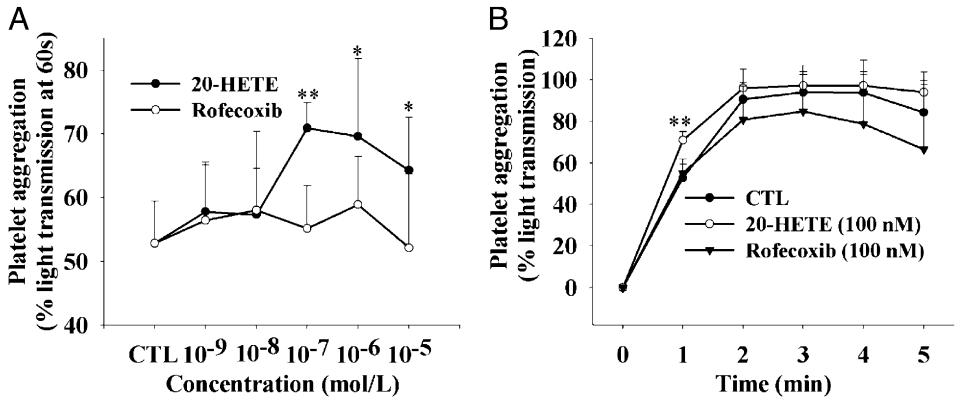


**Fig. 5.** 20-HETE but not rofecoxib accelerates ADP-induced rat platelet aggregation in vitro. (*A*) Aggregation percentage under a different concentration of rofecoxib or 20-HETE at 1 min after ADP was added. (*B*) Aggregation percentage tracing curve of ADP-induced platelet aggregation under $10^{-7}$ M 20-HETE or rofecoxib. Graphs represent the mean ± SEM, depicting the percentage of aggregation over 5 min ($n = 6$). The control (CTL) group contains neither rofecoxib nor 20-HETE. Each point represents the mean ± SD ($n = 6$). Statistical significance was determined by a two-sided unpaired *t* test and repeated measures one-way ANOVA (*$P < 0.05$; **$P < 0.01$).

phospholipase treatment and inhibits the ARA A23187- and U46619-induced human platelet aggregation at the concentrations of 10 and 30 μM, respectively, in a dose-dependent manner (29, 38). However, 20-HETE had no detectable agonist activity on human platelets at a concentration less than 30 μM (29). In contrast, 20-HETE was demonstrated to accelerate rat platelet aggregation significantly at a concentration between 100 nM and 10 μM in a dose-dependent and time-related manner in vitro (Fig. 5), whereas rofecoxib had no effect on platelet aggregation under the same conditions. In addition, an in vitro assay of blood clotting time showed that 20-HETE significantly increases the clotting tendency, whereas its COX-mediated metabolites 20-OH-$PGF_{2\alpha}$ and 20-OH-$PGE_2$ are similar to the control platelet aggregation (Fig. 4*A*). This indicates that 20-HETE is more detrimental to the vascular system than its COX-mediated metabolites. These data suggest that accumulation of 20-HETE contributes to the cardiovascular problems associated with a high dose of rofecoxib. This also cautions against the use of NSAIDs in patients with cardiovascular diseases, which was indicated by the clinical facts that NSAIDs, including rofecoxib, celecoxib, ibuprofen, diclofenac, and naproxen, increase mortality and cardiovascular morbidity in chronic heart failure (39).

The dramatic increase in 20-HETE observed with rofecoxib treatment seems more attributable to decreased degradation of 20-HETE than to increased production. These data link the accumulation of 20-HETE and shortened bleeding time to treatment with rofecoxib and related compounds. This dramatic increase in 20-HETE may, in turn, be linked to the adverse cardiovascular events of rofecoxib that may be shared with other nonaspirin NSAIDs. This hypothesis suggests 20-HETE as a biomarker for cardiovascular risk from coxibs as well as possible strategies for attenuation of their adverse effects. For example, we predict that inhibition or down-regulation of CYP4A and or CYP4F may ablate the cardiovascular events of coxibs. In addition, this study exemplifies metabolomic profiling as a promising tool to gain a more comprehensive understanding of biological processes.

## Materials and Methods

All procedures and animal care were performed in accordance with the protocols approved by the Institutional Animal Care and Use Committee of the University of California, Davis. Male C57BL/6 and Swiss Webster mice were purchased from Charles River Laboratories. Rofecoxib was purchased from Toronto Research Chemicals, Inc. PEG400, (2-hydroxypropyl)-β-cyclodextrin (HPCD), β-NADP sodium salt, and monoclonal anti-β-actin antibody were from Sigma–Aldrich. EDTA($K_3$) was purchased from Tyco Health Group LP. Water (>18.0 MΩ) was purified by a NANO pure system (Barnstead). ARA was purchased from Nu-Chek Prep, Inc. Glucose-6-phosphate dehydrogenase was purchased from MP Biomedicals, LLC. Calibrated capillary tubes (25 μL) were purchased from VWR International, LLC. Oxylipin standards and SC-560 were purchased from Cayman Chemical or synthesized in-house. Polyclonal anti-rat CYP4A antibody was purchased from Novus Biologicals. An Alzet miniosmotic pump (model 2004) was purchased from DURECT Corporation.

**Animal Protocol 1.** After acclimation for 1 wk in a standard animal facility, apparently healthy mice (C57BL/6, male, 9 wk of age) were randomly assigned to two equal groups ($n = 6$) and each mouse was housed in a separate cage with food and water available ad libitum. One group was administered rofecoxib (50 mg/L) that was suspended in drinking water containing 1% (vol/vol) PEG400 and 0.5% (wt/vol) HPCD for 3 mo, whereas another group was administered the drinking water containing 1% (vol/vol) PEG400 and 0.5% (wt/vol) HPCD as the control. The body weight, food intake, and water consumption of animals were monitored weekly during the investigation (results presented in Fig. S4). Bleeding time was measured in mice 15 min before they were killed. Mice were killed 3 mo after treatment. All samples were stored at −80 °C until analysis. Blood collection and plasma separation were performed for oxylipin analysis as described previously (40). The whole heart was removed after blood collection and weighed (results presented in Fig. S5).

***Measurement of tail bleeding time.*** The tail was placed in a horizontal position and kept at room temperature, and it was amputated 3 mm from the tip. Blood was blotted onto filter paper every 30 s. The time until no blood blot appeared on the filter paper was recorded as the bleeding time.

***Oxylipin profiling analysis.*** Oxylipin mediators were extracted from the murine plasma using the method described by Liu et al. (40) and were analyzed with LC-MS/MS as described previously (20).

**Animal Protocol 2.** After acclimation for 1 wk in a standard animal facility, apparently healthy mice (C57BL/6, male, 20 wk of age) were randomly assigned to two equal groups ($n = 6$) and each mouse was housed in a separate cage with food and water available ad libitum. One group was implanted s.c. with a miniosmotic pump loaded with 20-HETE, which was dissolved in a mixture of solvents [PEG400 (50% vol/vol) + DMSO (40% vol/vol) + ethanol (10% vol/vol)]. The infusion flow rate of 20-HETE was designed as 250 ng/h. Another group was implanted s.c. with a miniosmotic pump loaded with the vehicle alone. Bleeding time was measured in mice 30 min before they were killed. Mice were killed 3 wk after treatment. Blood collection and plasma separation were performed for oxylipin analysis as described by Liu et al. (40). All samples were stored at −80 °C until analysis.

**Animal Protocol 3: Measurement of Blood Clotting Time.** Prescored capillary tubes for blood collection were previously rinsed with DMSO, 20-HETE (0.5 mM in DMSO), 20-OH-$PGE_2$ (0.5 mM in DMSO), or 20-OH-$PGF_{2\alpha}$ (0.5 mM in DMSO). The final concentration of 20-HETE, 20-OH-$PGE_2$, and 20-OH-$PGF_{2\alpha}$ was calculated to be approximately 13 μM. Twenty-five microliters of venous blood was collected from the tail of Swiss Webster mice (male, 8 wk of age) after wiping off the first drop of blood. The capillary tube filled with the blood was immediately held between the palms to maintain it at body temperature for 2 min. The capillary tube was then broken off 1 cm from one end every 30 s and checked for the appearance of a thread of fibrin. The timer

was started when the blood was visible out of the tail and was stopped when a thin string of fibrin was seen. The time this took was regarded as the blood clotting time. Each compound was tested with blood from six individual mice.

**Incubation of Murine Liver S-9 Fraction.** Murine liver was from the pooled livers of the six mice in the control group (protocol 1). S-9 fractions were prepared according to the method described previously (41). The incubation was according to the modified method of Watanabe et al. (42). Specifically, 178 μL of S-9 fraction protein (0.28 mg/mL) was added to a 12-mm × 75-mm glass tube and incubated at 37 °C for 5 min. Then, 20 μL of the NADPH generating system (4 mg/mL) and 2 μL of ARA (10-μM final concentration) with or without rofecoxib (1-μM final concentration) were added to the tube. The whole reaction system was incubated at 37 °C for 2 h after 30 s of gentle mixing on a Vortex mixer ($n$ = 6). The reaction was quenched by the addition of 400 μL of methanol, followed by vigorous mixing for 15 s. The resulting solution (100 μL) was mixed with an equal volume of internal standard [200 nM 12-(3-cyclohexylureido)-dodecanoic acid in methanol]. After centrifugation at 20,800 × $g$ for 5 min, 50 μL of supernatant was transferred to analytical vials containing a 150-μL insert for oxylipin analysis, as described above.

The 20-HETE formation rate was determined by the incubation method described above. The pooled livers of the six mice in the control group and exposure to rofecoxib (protocol 1) were used. The incubation was terminated at 0, 0.25, 0.5, 1, 1.5, 2, 2.5, and 3 h after adding a NADPH generating system.

**Plasma Preparation and Hemostatic Coagulation Tests.** Venous blood was obtained from C57BL/6 mice (8–10 wk of age, male). The mice were anesthetized with sodium pentobarbital (1% water solution, 100 mg/kg administered i.p). About 0.7 mL of venous blood was collected from each mouse by suctioning from the right ventricle using a syringe containing sodium citrate.

Coagulation was blocked in the blood sample with 109 mmol/L sodium citrate (1:9 vol/vol), and the sample was then centrifuged at 2,400 × $g$ for 15 min to get platelet-free plasma. In this experiment, only fresh blood samples were used. All tests were completed within 2 h at room temperature. The plasma was incubated with different concentrations of rofecoxib or 20-HETE ranging from $10^{-9}$ to $10^{-5}$ M for exactly 3 min at 37 °C before being used for all measurements, which were performed by modifications of the conventional clinical procedures using a photoelectrical electromagnetism coagulometer (STEELLEX).

For testing PT, 50 μL of pretreated plasma was mixed with 100 μL of activating reagent at 37 °C. The coagulation time was then measured, and the INR was calculated by the coagulometer automatically. To measure TT, 100 μL of plasma was pretreated for 3 min at 37 °C; 100 μL of thrombin solution was then added, and coagulation time was measured. For the measurement of APTT, 50 μL of plasma and 50 μL of APTT reagent, which contained cephalin and ellagic acid, were mixed. After incubating for 3 min at 37 °C, 50 μL of 25-mmol/L $CaCl_2$ solution (37 °C) was added and coagulation time was measured. To measure the plasma FIB level, 90 μL of buffer and 10 μL of plasma were incubated for 3 min at 37 °C; 50 μL of activating reagent was then added, and the coagulation time was measured. The plasma FIB concentration (g/L) was calculated by the coagulometer automatically from a reference curve.

**Platelet Preparation and Aggregation Assays.** Venous blood was obtained from male Sprague–Dawley rats (180 ± 10 g). Preparation of platelet-rich plasma (PRP) and platelet-poor plasma (PPP) was performed as described previously (43). For the platelet aggregation assay, PRP was incubated in $10^{-9}$ to $10^{-5}$ M rofecoxib or 20-HETE at 37 °C in a photoelectrical turbidimetric platelet aggregometer (STEELLEX). Aggregation was induced by 5 μM ADP. Results were quantified by measurement of the rate or extent of change of light transmittance through the sample cuvette, and baseline transmittance was calibrated with the PPP.

**Immunoblot Analysis.** Western immunoblot analysis was performed using the methods detailed by Schmelzer et al. (7). Specifically, the microsomal proteins were isolated from the liver for CYP4A analysis. The proteins were separated by electrophoresis using 10% (wt/vol) SDS/PAGE and then transferred onto poly(vinylidene fluoride) membranes (Immobilon P; Millipore). CYP4A-like proteins were detected with polyclonal antibodies raised to rat CYP4A from Novus Biologicals, and β-actin was detected with monoclonal antibody from Sigma–Aldrich. The membranes were incubated with an HRP-linked IgG whole secondary antibody (Amersham Pharmacia Biosciences) at 1:5,000 dilutions and then washed. Secondary antibodies were visualized by a SuperSignal West Femto Substrate chemiluminescence detection system (Pierce) and detected by autoradiography. The experiment was replicated with independent livers. The gels were scanned, and the CYP4A1 reactive bands were expressed as a ratio with β-actin. Single bands were detected.

**Measurement of Cytokines.** Plasma levels of FIB and PF-4 were measured using a Mouse Fibrinogen ELISA Kit (Innovative Research) and a Mouse PF-4 ELISA kit (RayBiotech) according to the manufacturers' instructions. Briefly, the plasma was thawed and added to 96-well plate precoated with immobilized antibody and was incubated for 2.5 h at room temperature. The wells were washed, and biotinylated anti-mouse fibrinogen or PF-4 antibody was added and incubated at room temperature for 30 min. Following three additional washes, the plates were incubated for 30 min with HRP-conjugated streptavidin. The wells were washed again, and a tetramethylbenzidine substrate solution was added to the wells and developed for 30 min. The enzyme reaction was stopped by the addition of the stop reagent. The absorbance of each well was measured at 450 nm. A linear standard calibration curve was constructed by plotting the absorbance of the standards. The FIB and PF-4 concentrations in each sample were determined from the detectable ranges of the linear calibration curve.

**Statistics.** Data are presented as means ± SD. Data were analyzed with a two-sided unpaired $t$ test and one-way ANOVA, and $P < 0.05$ was considered significant.

**ACKNOWLEDGMENTS.** This work was supported, in part, by National Institute of Environmental Health Sciences Grant ES02710, National Institute of Environmental Health Sciences Superfund P42 ES04699, National Heart, Lung, and Blood Institute Grants HL85727 and HL85844, a Major National Basic Research Grant of China (2010CB912504), the Elizabeth Nash Memorial fellowship from the Cystic Fibrosis Foundation, Inc. (to J.Y.), a Veterans Affairs merit review grant (to N.C.) and American Heart Association Western Affiliates postdoctoral fellowship award (to H.Q.). B.D.H. is a George and Judy Marcus Senior Fellow of the American Asthma Foundation.

1. Mukherjee D, Nissen SE, Topol EJ (2001) Risk of cardiovascular events associated with selective COX-2 inhibitors. *JAMA* 286:954–959.
2. Bombardier C, Laine L, Reicin A, Shapiro D, Burgos-Vargas R, et al. (2000) Comparison of upper gastrointestinal toxicity of rofecoxib and naproxen in patients with rheumatoid arthritis. VIGOR Study Group. *New Engl J Med* 343:1520–1528.
3. Wadman M (2007) Merck settles Vioxx lawsuits for $4.85 billion. *Nature* 450:324–325.
4. Ray WA, Griffin MR, Stein CM (2004) Cardiovascular toxicity of valdecoxib. *N Engl J Med* 351:2767.
5. Cheng Y, et al. (2002) Role of prostacyclin in the cardiovascular response to thromboxane A2. *Science* 296:539–541.
6. Fitzgerald GA (2004) Coxibs and cardiovascular disease. *N Engl J Med* 351:1709–1711.
7. Schmelzer KR, et al. (2006) Enhancement of antinociception by coadministration of nonsteroidal anti-inflammatory drugs and soluble epoxide hydrolase inhibitors. *Proc Natl Acad Sci USA* 103:13646–13651.
8. Hippisley-Cox J, Coupland C (2005) Risk of myocardial infarction in patients taking cyclo-oxygenase-2 inhibitors or conventional non-steroidal anti-inflammatory drugs: Population based nested case-control analysis. *BMJ* 330:1366–1369.
9. Singh G, Wu O, Langhorne P, Madhok R (2006) Risk of acute myocardial infarction with nonselective non-steroidal anti-inflammatory drugs: A meta-analysis. *Arthritis Res Ther* 8:R153.
10. Helin-Salmivaara A, et al. (2006) NSAID use and the risk of hospitalization for first myocardial infarction in the general population: A nationwide case-control study from Finland. *Eur Heart J* 27:1657–1663.
11. Johnson AG, Simons LA, Simons J, Friedlander Y, McCallum J (1993) Non-steroidal anti-inflammatory drugs and hypertension in the elderly: A community-based cross-sectional study. *Br J Clin Pharmacol* 35:455–459.
12. Page J, Henry D (2000) Consumption of NSAIDs and the development of congestive heart failure in elderly patients: An underrecognized public health problem. *Arch Intern Med* 160:777–784.
13. Reddy LR, Corey EJ (2005) Facile air oxidation of the conjugate base of rofecoxib (Vioxx (TM)), a possible contributor to chronic human toxicity. *Tetrahedron Lett* 46: 927–929.
14. Brindle JT, et al. (2002) Rapid and noninvasive diagnosis of the presence and severity of coronary heart disease using 1H-NMR-based metabonomics. *Nat Med* 8:1439–1444.
15. Lewis GD, et al. (2008) Metabolite profiling of blood from individuals undergoing planned myocardial infarction reveals early markers of myocardial injury. *J Clin Invest* 118:3503–3512.
16. Lindon JC, et al. (2005) The Consortium for Metabonomic Toxicology (COMET): Aims, activities and achievements. *Pharmacogenomics* 6:691–699.
17. Fiehn O (2002) Metabolomics—The link between genotypes and phenotypes. *Plant Mol Biol* 48:155–171.
18. Wikoff WR, Pendyala G, Siuzdak G, Fox HS (2008) Metabolomic analysis of the cerebrospinal fluid reveals changes in phospholipase expression in the CNS of SIV-infected macaques. *J Clin Invest* 118:2661–2669.
19. Liu JY, et al. (2010) Inhibition of soluble epoxide hydrolase enhances the anti-inflammatory effects of aspirin and 5-lipoxygenase activation protein inhibitor in a murine model. *Biochem Pharmacol* 79:880–887.
20. Yang J, Schmelzer K, Georgi K, Hammock BD (2009) Quantitative profiling method for oxylipin metabolome by liquid chromatography electrospray ionization tandem mass spectrometry. *Anal Chem* 81:8085–8093.

21. Tofler GH, et al. (1987) Concurrent morning increase in platelet aggregability and the risk of myocardial infarction and sudden cardiac death. *N Engl J Med* 316:1514–1518.
22. Kovalenko VM, et al. (1991) The blood-coagulation and anticoagulation system and platelet-aggregation at rest and exercise in healthy-persons and patients with coronary heart-disease. *Ter Arkh* 63:69–71 (in Russian).
23. Hurlen M, Seljeflot I, Arnesen H (2000) Increased platelet aggregability during exercise in patients with previous myocardial infarction. Lack of inhibition by aspirin. *Thromb Res* 99:487–494.
24. Kalendov Z, Austin J, Steele P (1974) Increased platelet aggregability in young patients with stroke. *Neurology* 24:373.
25. Milner PC, Martin JF (1985) Shortened bleeding time in acute myocardial infarction and its relation to platelet mass. *Br Med J (Clin Res Ed)* 290:1767–1770.
26. Dalby Kristensen S, Milner PC, Martin JF (1988) Bleeding time and platelet volume in acute myocardial infarction—A 2 year follow-up study. *Thromb Haemost* 59:353–356.
27. Sciulli MG, Capone ML, Tacconelli S, Patrignani P (2005) The future of traditional nonsteroidal antiinflammatory drugs and cyclooxygenase-2 inhibitors in the treatment of inflammation and pain. *Pharmacol Rep* 57(Suppl):66–85.
28. Powell PK, Wolf I, Jin RY, Lasker JM (1998) Metabolism of arachidonic acid to 20-hydroxy-5,8,11, 14-eicosatetraenoic acid by P450 enzymes in human liver: Involvement of CYP4F2 and CYP4A11. *J Pharmacol Exp Ther* 285:1327–1336.
29. Hill E, Fitzpatrick F, Murphy RC (1992) Biological activity and metabolism of 20-hydroxyeicosatetraenoic acid in the human platelet. *Br J Pharmacol* 106:267–274.
30. Schwartzman ML, Falck JR, Yadagiri P, Escalante B (1989) Metabolism of 20-hydroxyeicosatetraenoic acid by cyclooxygenase. Formation and identification of novel endothelium-dependent vasoconstrictor metabolites. *J Biol Chem* 264:11658–11662.
31. Fang X, et al. (2006) 20-Hydroxyeicosatetraenoic acid is a potent dilator of mouse basilar artery: Role of cyclooxygenase. *Am J Physiol-Heart C* 291:H2301–H2307.
32. Collins XH, et al. (2005) Omega-oxidation of 20-hydroxyeicosatetraenoic acid (20-HETE) in cerebral microvascular smooth muscle and endothelium by alcohol dehydrogenase 4. *J Biol Chem* 280:33157–33164.
33. Roman RJ, Renic M, Dunn KMJ, Takeuchi K, Hacein-Bey L (2006) Evidence that 20-HETE contributes to the development of acute and delayed cerebral vasospasm. *Neurol Res* 28:738–749.
34. Miyata N, et al. (2005) Beneficial effects of a new 20-hydroxyeicosatetraenoic acid synthesis inhibitor, TS-011 [N-(3-chloro-4-morpholin-4-yl) phenyl-N′-hydroxyimido formamide], on hemorrhagic and ischemic stroke. *J Pharmacol Exp Ther* 314:77–85.
35. Kehl F, et al. (2002) 20-HETE contributes to the acute fall in cerebral blood flow after subarachnoid hemorrhage in the rat. *Am J Physiol-Heart C* 282:H1556–H1565.
36. Nithipatikom K, et al. (2004) Inhibition of cytochrome P450omega-hydroxylase: A novel endogenous cardioprotective pathway. *Circ Res* 95:e65–e71.
37. Escalante B, et al. (1993) 20-hydroxyeicosatetraenoic acid is an endothelium-dependent vasoconstrictor in rabbit arteries. *Eur J Pharmacol* 235:1–7.
38. Zhu Y, Schieber EB, McGiff JC, Balazy M (1995) Identification of arachidonate P-450 metabolites in human platelet phospholipids. *Hypertension* 25:854–859.
39. Gislason GH, et al. (2009) Increased mortality and cardiovascular morbidity associated with use of nonsteroidal anti-inflammatory drugs in chronic heart failure. *Arch Intern Med* 169:141–149.
40. Liu JY, et al. (2009) Pharmacokinetic optimization of four soluble epoxide hydrolase inhibitors for use in a murine model of inflammation. *Br J Pharmacol* 156:284–296.
41. Bauer C, Corsi C, Paolini M (1994) Stability of microsomal monooxygenases in murine liver S9 fractions derived from phenobarbital and beta-naphthoflavone induced animals under various long-term conditions of storage. *Teratog Carcinog Mutagen* 14:13–22.
42. Watanabe T, Morisseau C, Newman JW, Hammock BD (2003) In vitro metabolism of the mammalian soluble epoxide hydrolase inhibitor, 1-cyclohexyl-3-dodecyl-urea. *Drug Metab Dispos* 31:846–853.
43. Pawloski JR, Swaminathan RV, Stamler JS (1998) Cell-free and erythrocytic S-nitrosohemoglobin inhibits human platelet aggregation. *Circulation* 97:263–267.